ABSTRACT

FARTHING, AMY LYNN. Characterization of Parvalbumin Interneurons and Validation of PV-IRES-Cre Recombination in the Basolateral Amygdala. (Under the direction of Drs. Elizabeth Lucas and Emilie Rissman).

The basolateral amygdala (BLA) plays an essential role in processing emotionally-salient stimuli and governing behavioral outputs. The BLA is composed of 80% glutamatergic projection neurons and 20% GABAergic interneurons. Parvalbumin (PV) interneurons constitute roughly half of the GABAergic population and are preferentially surrounded by extracellular matrix glycoproteins, perineuronal nets (PNNs). Previous studies have documented the density of BLA PV cells surrounded by PNNs in male and female rodents; however, to date, there has been no report of density changes across the female rodent estrous cycle, a 4-5 day window of time characterized by rapid fluctuations in ovarian hormone concentrations. Herein using mice, I determined the density and proportion of PV cells surrounded by PNNs by conducting immunofluorescence on BLA sections from gonadal-intact males, females in diestrus 1 (the low ovarian hormone state), and females in proestrus (the high ovarian hormone state). Quantifications were assessed in the PV-IRES-Cre mouse line crossed to $Ai9^{+/+}$ reporter mice to confer tdTomato expression in PV interneurons. In addition to analyzing the PV/PNN population, I also assessed Cre recombination efficiency and specificity in the BLA, as no studies have independently assessed these factors in males and females. I observed the density of BLA PV/PNN-expressing cells did not depend on sex or estrous cycle stage and BLA PV-IRES-Cre recombination efficiency and specificity is equivalent in males and females. Therefore, my findings suggest that future studies can reliably use PV-IRES-Cre dependent recombination tools within the BLA of mice to examine potential sex differences that may exist for GABAergic signaling.

Characterization of Parvalbumin Interneurons and Validation of PV-IRES-Cre Recombination in the Basolateral Amygdala

by
Amy Lynn Farthing

A thesis submitted to the Graduate Faculty of
North Carolina State University
in partial fulfillment of the
requirements for the degree of
Master of Science

Comparative Biomedical Sciences

Raleigh, North Carolina
2022

APPROVED BY:

_____	_____
Elizabeth Lucas Committee Co-Chair	Emilie Rissman Committee Co-Chair
_____	_____
John Meitzen	Casey Nestor

BIOGRAPHY

Amy Farthing was raised in Park Forest, IL, a south suburb of Chicago. She attended Augustana College in Rock Island, IL, and later graduated with a BA in Biology and a minor in Biochemistry. Following graduation, she pursued multiple internships across the country. She interned at a white-tailed deer ranch in Texas and an animal sanctuary in Alabama. She also worked as a seasonal biological technician for USGS monitoring piping plover populations in North Dakota. Although Amy learned fieldwork was not her forte, she enjoyed contributing to scientific research. She then went on to earn a MS in Agricultural and Natural Resource Sciences from Tarleton State University. Her Master's research sought to determine the effects of gossypol on Northern bobwhite quail. Amy thoroughly enjoyed her Master's research and sought additional opportunities to learn about conducting toxicological research. Upon moving to North Carolina, Amy worked as an ORISE post-master's intern at the US EPA in Research Triangle Park. While she was there, she worked in the labs of Dr. Neil Chernoff and Dr. David Thomas. Her passion for conducting research and desire to gain additional research skills prompted her to apply to PhD programs. Amy was accepted into the Comparative Biomedical Research Program at NCSU, and after seven months of rotating in different labs, she joined the lab of Dr. Elizabeth Lucas, right before the COVID-19 pandemic hit the world. Her project focused on estrous cycle regulation of parvalbumin interneurons in the basolateral amygdala. Due to unforeseen circumstances, rather than continuing with the PhD, Amy ultimately decided to transfer to the CBS Master's program. Although life does not always go as expected, Amy is very grateful for the mentorship Beth Lucas has provided; her dedication to Amy's personal and professional advancement has made her into a better person and scientist. The skills gained during her time in the Lucas lab have allowed her to pursue her next opportunity as a research assistant for a lab at the NIH.

TABLE OF CONTENTS

LIST OF TABLES

LIST OF FIGURES

CHAPTER 1

Abstract

The basolateral amygdala (BLA) plays an essential role in processing emotionally-salient stimuli and governing behavioral outputs. The BLA is composed of 80% glutamatergic projection neurons and 20% GABAergic interneurons. Parvalbumin (PV) interneurons constitute roughly half of the GABAergic population and are preferentially surrounded by extracellular matrix glycoproteins, perineuronal nets (PNNs). Previous studies have documented the density of BLA PV cells surrounded by PNNs in male and female rodents; however, to date, there has been no report of density changes across the female rodent estrous cycle, a 4–5 day window of time characterized by rapid fluctuations in ovarian hormone concentrations. Herein using mice, I determined the density and proportion of PV cells surrounded by PNNs by conducting immunofluorescence on BLA sections from gonadal-intact males, females in diestrus 1 (the low ovarian hormone state), and females in proestrus (the high ovarian hormone state). Quantifications were assessed in the PV-IRES-Cre mouse line crossed to Ai9$^{+/+}$ reporter mice to confer tdTomato expression in PV interneurons. In addition to analyzing the PV/PNN population, I also assessed Cre recombination efficiency and specificity in the BLA, as no studies have independently assessed these factors in males and females. I observed the density of BLA PV/PNN-expressing cells did not depend on sex or estrous cycle stage and BLA PV-IRES-Cre recombination efficiency and specificity is equivalent in males and females. Therefore, my findings suggest that future studies can reliably use PV-IRES-Cre dependent recombination tools within the BLA of mice to examine potential sex differences that may exist for GABAergic signaling.

Introduction

Generally known as the "sensory gateway to the emotions," the amygdala is an evolutionally conserved brain region involved in assigning negative or positive valance to emotionally-salient stimuli (Aggleton and Mishkin, 1986). The amygdala is composed of more than a dozen nuclei, each of which have distinct cellular populations and connections (Johnston, 1923). One particularly important nucleus is the basolateral amygdala (BLA), which is divided into the lateral and basal regions and controlled by cortical and thalamic neurons that project to the BLA to convey sensory information (Johnston, 1923; LeDoux et al., 1990; McDonald, 1998). Projections from the BLA to the central amygdala, bed nucleus of the stria terminalis, and ventral striatum then activate the hypothalamus and brainstem to induce emotionally-driven behavioral outputs (McDonald, 1991).

The BLA is primarily composed of two major cell classes: long-range, glutamatergic projection neurons and non-principal neurons, most of which are locally projecting, GABAergic interneurons (McDonald, 1984; McDonald, 1992). Projection neurons constitute approximately 80% of BLA neurons while non-principal neurons make up 20% (McDonald, 1992; Sah et al. 2003). Neurons comprising the non-principal population are heterogenous and are often characterized by expression of calcium-binding proteins (parvalbumin (PV), calbindin, or calretinin) and neuropeptides (somatostatin, cholecystokinin, or vasoactive intestinal peptide) (McDonald, 2020). Out of these cellular subpopulations, PV-expressing interneurons constitute the majority, making up 41% of the total GABAergic population in rodents (McDonald and Mascagni, 2001; Mascagni and McDonald, 2003).

PV interneurons are involved regulating the critical excitatory to inhibitory balance in the BLA, as their fast-firing action potential generation tightly regulates the activity of projection neurons through feedforward and feedback inhibition (Ferguson and Gao 2018; Lucas and Clem, 2018). Maturation of PV interneurons corresponds to closure of critical periods in many brain regions, including the BLA, and has been linked to expression of perineuronal nets (PNNs) (Gogolla et al., 2009; Baker et al., 2017; Carulli and Verhaagen, 2021). PNNs, which primarily surround PV interneurons, are extracellular matrix glycoproteins that form around proximal dendrites, cell bodies, and axon initial segments of neurons in a lattice-like matter (Sorg et al., 2016). PNNs have a robust role in regulating PV interneuron plasticity through a variety of mechanisms including AMPA receptor trafficking, maintenance of ion-buffering, and restriction of synaptic connections (Härtig et al., 1999; Deepa et al., 2002; Frischknecht et al., 2009; Morawski et al., 2015).

Moreover, previous studies have found PV interneurons express the ovarian hormone receptor, estrogen receptor β (ERβ), in many brain regions including the BLA (Blurton-Jones and Tuszynski, 2002; Kritzer, 2002; Sárvári et al., 2010; Mo et al., 2015; Clemens et al., 2019). ERβ is a nuclear receptor that is activated by exogenous and endogenous estrogens, including 17β-estradiol, the primary circulating estrogen during the female estrous cycle (Freeman, 1994; Kuiper et al., 1996). The rodent estrous cycle is divided into four stages, proestrus, estrus, diestrus 1, and diestrus 2, and is tightly regulated by the light-dark cycle (Freeman, 1994; Ajayi and Akhigbe, 2020). Rodents on a 12 hr light/dark cycle experience maximum levels of 17β-estradiol during the late morning to early afternoon and progesterone during the evening of proestrus, the pre-ovulatory phase (Butcher et al., 1974; Smith et al., 1975; Freeman, 1994). Low stable levels of 17β-estradiol and progesterone are secreted during estrus, the period of sexual receptivity and ovulation (Butcher

et al., 1974; Smith et al., 1975; Freeman, 1994). Diestrus 1 is characterized by a gradual rise in progesterone and low concentration of 17β-estradiol while diestrus 2 is linked to a rapid decline in progesterone and progressive rise in 17β-estradiol (Butcher et al., 1974; Smith et al., 1975; Freeman, 1994)

Since female mammals experience cyclic changes in concentrations of 17β-estradiol and other ovarian hormones, it suggests PV interneurons are modulated differently across the reproductive cycle. Few studies have examined the female rodent estrous cycle on PV interneurons (Blume et al., 2017; Clemens et al., 2019). Indeed, Clemens et al. (2019) found the firing rate of layer V barrel cortical PV interneurons from rats was regulated by the estrous cycle in an ERβ-dependent mechanism wherein PV interneurons had increased ongoing firing rates during proestrus and estrus compared to diestrus 1 and 2 (Clemens et al., 2019). Furthermore, *in vivo* and *in vitro* application estradiol after ovariectomy replicated the increased firing rate while application of PHTPP, an ERβ antagonist, prevented the effect (Clemens et al., 2019). Similarly, Blume et al. (2017) determined BLA PV interneurons are regulated differently between males and females and across the female rodent estrous cycle. The frequency of spontaneous inhibitory post-synaptic currents onto putative PV cells from rats was higher in females compared to males and in diestrus 1 females compared to those in proestrus (Blume et al., 2017). Additionally, the amount of BLA PV-expressing cells in was higher in males compared to females and higher in diestrus than proestrus females (Blume et al., 2017).

Despite evidence of sex and estrous cycle dependent differences, to date no studies reported differences in the density of BLA PV cells expressing PNNs across the estrous cycle. My first aim was to characterize the subpopulation of PV cells expressing PNNs in the BLA from males and females in diestrus 1 and proestrus. I quantified these differences using a Cre-dependent transgenic

mouse line in which PV interneurons were selectively labeled by the fluorescent protein, tdTomato (Hippenmeyer et al., 2005; Madisen et al., 2010). In addition to analyzing the PV/PNN population, I also assessed Cre recombination efficiency and specificity by examining the density of BLA PV cells expressing tdTomato and vice versa. Currently, no studies have independently assessed Cre recombination efficiency and specificity in PV-IRES-Cre male and female mice. This is an important aspect to consider if future studies want to use this mouse line to examine sex differences based on Cre-dependent experimental manipulations.

Materials and Methods

Animals.

All experiments were approved by the Institutional Animal Care and Use Committee at North Carolina State University (#20-520-B). The following mouse lines were ordered from Jackson Laboratories (Bar Harbor, ME), maintained on a C57Bl/6J background, and crossed to selectively induce Cre-dependent expression of tdTomato in PV cells: PV-IRES $Cre^{+/+}$ (Stock #017320) and Rosa-CAG-LSL-tdTomato-WPRE ($Ai9^{+/+}$; Stock #007909). Mice were housed by sex with 2-4 per cage in a temperature and humidity-controlled vivarium with a 12 hr light/dark cycle (lights on/off at 8 am/8 pm). Food (5001 rodent laboratory chow; Purina, St. Louis, MO) and water were provided *ad libitum* throughout all experiments. All experiments were conducted on litter-matched, gonadally-intact male and female PV-IRES-$Cre^{+/-}$;$Ai9^{+/-}$ mice between 60-80 days of age (see Fig. 1 for experimental pipeline).

Estrous Cycle Monitoring.

Estrous cycle stage was determined by categorization of vaginal cytology as previously described (Allen et al., 1924). Briefly, cells were collected daily from each animal between 9 and 10 am via a vaginal lavage with 50 µL of 0.9% normal saline (Cat. #L97753; Fisher Scientific, Waltham,

MA) using a pipette. Vaginal cytology was visualized with hematoxylin (Cat. #NC9220898; Fisher Scientific) and eosin-y (Cat. #50420842; Fisher Scientific) staining. Estrous cycle stage was categorized as follows: diestrus with presence of leukocytes, proestrus with dividing nucleated epithelial cells, or estrus with cornified cells (Cora et al., 2015). Females were monitored daily until they had at least two complete, consecutive cycles and euthanized in either diestrus 1 (low ovarian hormone state) or proestrus (high ovarian hormone state). Females were excluded if they had an irregular cycle (n = 4), characterized by being stuck in the same stage for 5 or more days. Males underwent mock lavage, consisting of restraint and gently rubbing a pipette tip on the scrotum for 5-10 sec, to account for the additional handling received by females.

Perfusion and Tissue Sectioning.

All mice were anesthetized with an intraperitoneal injection of 2.5% Avertin (500 mg/kg; Fischer Scientific) prior to transcardial perfusion with 0.1M phosphate buffered saline (PBS) and 4% paraformaldehyde (PFA) made with PBS. All perfusions took place between 3 to 4 pm. Following perfusion, brains were removed and postfixed overnight in 4% PFA, washed 3 times in PBS, and stored in PBS with 0.2% sodium azide (NaN_3) at 4ºC until all experimental brains were harvested. Brains were sectioned with a vibratome (VT1000S; Leica Biosystems, Deer Park, IL) on the coronal plane at 50 μm and stored in a solution of glycerol (Cat. #G334; Fischer Scientific) with 0.2% NaN_3 at -20ºC. Poorly perfused or sectioned brains were excluded from analysis (n = 4; 1 male and 3 females in diestrus 1).

Immunofluorescence.

Immunofluorescence staining was conducted on floating sections containing anterior, medial, and posterior BLA as previously described (Lucas et al., 2016) (n = 7 males, 4 females in diestrus 1, and 7 females in proestrus). After washes in PBS, slices were blocked with 10% normal donkey

serum (Cat. #017-000-121; Jackson ImmunoResearch, West Grove, PA) for 1 hr at room temperature prior to overnight incubation in a primary cocktail with 0.1% Triton-X (Cat. #BP151-500; Fischer Scientific) PBS with 5% normal donkey serum at 4ºC. Primary antibodies included rabbit anti-PV (1:1000, Cat. #PV-27; Swant, Burgdorf, Switzerland) and mouse anti-glutamic acid decarboxylase 67 (1:500, Cat. #MAB5406, clone 1G10.2; Millipore, Burlington, MA; GAD67) (Table 1). Biotinylated *Wisteria floribunda* lectin (1:100, Cat. #B-1355-2; Vector Labs, Burlingame, CA; WFL) was used to stain chondroitin sulfate proteoglycans, the primary scaffold of PNNs (Table 1). Following washes in PBS, slices were incubated in a secondary cocktail with 0.1% Triton-X PBS with 5% donkey serum for 2 hr at room temperature. Fluorescence-conjugated secondary antibodies included donkey raised anti-mouse Alexa Fluor 647 (1:500, Cat. #711-605-152; Jackson ImmunoResearch) and anti-rabbit DyLight 405 (1:200, Cat. #715-475-150; Jackson ImmunoResearch) (Table 1). Streptavidin conjugated Alexa Fluor 488 (1:100, Cat. #016-540-084; Jackson ImmunoResearch) labeled biotinylated *Wisteria floribunda* lectin expressing PNNs (Table 1). Slices were washed in PBS, mounted onto slides, and coversliped with Prolong Antifade Gold (Cat. # P36930; Fischer Scientific).

Antibody and Lectin Characterization.

The polyclonal PV antibody was raised in rabbit against recombinant rat PV. Filice et al. (2017) confirmed via Western blot the presence of a single band at ~12 kDa, the molecular weight of PV in brain extracts from wild-type (WT) mice that was absent in PV-knockout (KO) mice. The specificity was further validated via immunofluorescence, where the antibody labeled PV neurons in WT but not PV-KO mice (Filice et al., 2017). The monoclonal GAD67 antibody was raised in mouse against recombinant his-tag-containing human GAD67 protein. According to the manufacturer, the antibody detects a single band at 67 kDa, corresponding to the GAD67 isoform

rather than the GAD65 isoform, on Western blots from rats, mice, and humans. The staining pattern we observed was similar to GAD67 immunostaining in the amygdala by Morena et al. (2019) and McDonald and Mott (2021). Biotinylated WFL binds to chondroitin sulfate proteoglycans terminating in *N*-acetyl-D-galactosamine with a preference for β glycosidic linkage (Kurokawa et al. 1976). Specificity of WFL has been validated via enzymatic digestion of the proteoglycans, which prevents immunolabeling (Galtrey and Fawcett, 2007; Pantazopoulos et al., 2010; Pantazopoulos et a., 2020). We further validated WFL staining by omitting WFL or streptavidin conjugated Alexa Fluor 488, which resulted in no signal.

Microscopy and Image Quantification.

Images were taken of the left and right hemisphere from an anterior (bregma -0.82 to -1.34), medial (bregma -1.46 to -1.94), and posterior (bregma -2.06 to -2.46) section containing the BLA; a total of 6 images were captured per animal. Only one animal, a female in diestrus 1, lacked a medial right BLA section and had 5 sections, rather than 6. Images were taken using an Olympus FV3000 confocal laser scanning microscope equipped with an Olympus UPlan Super Apochromat 20X/0.75 objective. Fluorophore absorption and emission settings included the following: 405 nm and 410-450 nm for GAD67, 561 nm and 570-670 nm for tdTomato, 488 nm and 500-540 nm for PNNs, and 640 nm and 650-750 nm for PV. The laser power, voltage, gain and offset were held constant throughout imaging. Laser power was set so <20% pixels/cell were saturated. Images were acquired with a multi-alkali coated photomultiplier and Fluoview 3000 acquisition software. Stitched z-plane stacks were taken of the top 20 μm for each BLA section using a step-size of 2 μm and scan size of 1024x1024. Z-plane maximum intensity projections were collected from each stitched image and used for quantification. Images were uploaded into ImageJ (version 1.53; NIH, Bethesda, MD) using the Bioformats plugin. Regions of interest were manually drawn around each

BLA and the area was recorded. Manual quantification of single, double, triple, and quadruple-labeled cells was performed blinded using the Cell Counter plugin. Quantification of PNNs exhibiting glia morphology were excluded from analysis.

Statistical Analysis.

All statistical analyses were conducted with GraphPad Prism IX (La Jolla, CA, USA). Briefly, the area and cell counts for each BLA were averaged to obtain an overall average per animal. The number single, double, tripled, and quadruple-labeled cells was divided by the area (mm^2) to calculate the density. To further evaluate the cellular populations, I determined the proportion of cells co-expressing double, triple, or quadruple-labeled markers. Proportions were calculated as the (cell count of double, triple, or quadruple-labeled cells / cell count of single-labeled cells)*100). An unpaired two-tailed *t*-test was performed on the overall averages to assess statistical differences between males vs females and diestrus 1 vs proestrus females. If data violated assumptions of normality or homogeneity of variance, a non-parametric Mann Whitney U or Welch's *t*-test was performed. A p-value of <0.05 was considered significant. All data are presented as mean $\pm$ standard error of the mean (SEM).

Results

Characterization of PV Expressing Cells in the BLA.

Using immunofluorescence, I observed robust staining of PV, GAD67, and PNN-expressing cells in the BLA (Fig. 2A-B). There were no differences ($p > 0.05$) in the density (cell count/mm^2) of cellular populations expressing PV, PV/GAD67, PNNs, PV/PNNs, Non-PV/PNNs, or PV/GAD67/PNNs in the BLA between sexes or between stages of the estrous cycle in females (Table 2). Due to these results, I combined densities for males and females (Fig. 2C). Specifically, I found 88.11% of PV cells expressed GAD67, 35.70% were surrounded by PNNs, and 31.90%

expressed GAD67 and were surrounded by PNNs (Fig. 3A). When stratifying the ratio of PV cells that expressed GAD67 and/or PNNs by sex and estrous cycle stage, no differences were found ($p > 0.05$) (Table 3).

In addition to evaluating the PV subpopulation expressing PNNs, I also assessed the PNN subpopulation expressing PV. Evaluation of PNN-expressing cells revealed 50.75% of PNNs surround non-PV expressing cells, leaving 49.25% surrounding PV cells (Fig. 3B). A total of 43.90% of PNNs surrounded PV cells that also expressed GAD67 (Fig. 3B). While there were no sex or estrous cycle effects on the proportion of PNNs surrounding non-PV and PV expressing cells ($p > 0.05$), there was a difference between males and females in the percentage of PNNs that surrounded PV cells that also expressed GAD67 ($t_{16} = 2.146$, $p = 0.0475$) (Table 3). The ratio of PNNs surrounding PV/GAD67 cells was lower in females ($41.18 \pm 2.13\%$) compared to males ($48.17 \pm 2.32\%$); there was no effect of estrous cycle on this parameter ($p > 0.05$) (Table 3).

Validation of PV-IRES-Cre Recombination.

I saw robust labeling of tdTomato-expressing cells in the BLA, indicating these cells underwent Cre recombination (Fig. 2A-B). The density (cell count/mm^2) of cellular populations expressing tdTomato, tdTomato/PV, tdTomato/GAD67, tdTomato/PV/GAD67, tdTomato/PNNs, tdTomato/PV/PNNs, and tdTomato/PV/GAD67/PNNs in the BLA showed no sex or estrous cycle dependent differences ($p > 0.05$) (Table 2). Due to these results, I combined densities for males and females (Fig. 2C).

To assess PV-IRES-Cre recombination specificity, I examined the proportion of tdTomato cells that expressed PV. I found 91.58% of tdTomato cells expressed PV, 84.13% expressed GAD67, and 80.13% co-expressed PV and GAD67 (Fig. 4A). When I broke these data down by sex and estrous cycle, I found no effect on the proportion of tdTomato cells that expressed

PV ($p > 0.05$) (Table 4). There were sex differences in ratio of tdTomato cells that expressed GAD67 and co-expressed PV and GAD67 (Table 4). The ratio of tdTomato cells that express GAD67 ($t_{16} = 2.145$, $p = 0.0477$) and PV/GAD67 ($t_{16} = 2.195$, $p = 0.0433$) was less in females (81.89 ± 1.79; $77.44 \pm 2.27\%$) compared to males (87.65 ± 1.84; $84.36 \pm 1.65\%$) (Table 4). There was no effect of estrous cycle on these variables ($p > 0.05$) (Table 4).

To determine PV-IRES-Cre recombination efficiency, I analyzed the ratio of PV cells expressing tdTomato. Analysis of the PV population showed only 42.96% of PV cells expressed tdTomato and 37.48% expressed tdTomato and GAD67 (Fig. 4B). Similar to the percentage of PV cells that expressed GAD67 and/or PNNs, there were no sex or estrous cycle effects on the ratio that expressed tdTomato or tdTomato and GAD67 ($p > 0.05$) (Table 4).

Although not directly related to recombination specificity and efficiency rate, I further examined the proportion of tdTomato and PV cells co-expressing PNNs with additional markers (Fig. 4A-B). Specifically, 48.39% of tdTomato cells were surrounded by PNNs, 46.34% co-expressed PV and PNNs, and 41.30% expressed PV, GAD67, and PNNs (Fig. 4A). Examination of the PV population revealed 21.80% of PV cells expressed tdTomato and PNNs while 19.36% co-expressed tdTomato, GAD67, and PNNs (Fig. 4B). I similarly determined the ratio of PNNs co-expressing tdTomato and PV. I found 31.70% of PNNs surrounded tdTomato cells, 30.33% surrounded PV cells that also expressed tdTomato, and 26.88% were found around cells expressing PV, tdTomato, and GAD67 (Fig. 4C). There were no sex or estrous cycle effects on any of the parameters mentioned above ($p > 0.05$) (Table 4).

Discussion

This is the first study to examine estrous cycle differences on the density of BLA PV cells ensheathed by PNNs and to assess Cre recombination efficiency and specificity in PV-IRES-Cre

male and female mice. Overall, my results indicate there are no estrous cycles differences in the density of BLA PV cells surrounded by PNNs or sex differences in PV-IRES-Cre recombination efficiency and specificity. I decided to focus on BLA PV cells for multiple reasons. PV-expressing cells are the primary cell type surrounded by PNNs, and PNNs have a role in mediating firing properties of PV cells (Härtig et al., 1992; Dityatev et al., 2007; Balmer, 2016; Favuzzi et al., 2017). It has also been documented that PV cells express ERβ, one of the main estrogen receptors (Blurton-Jones and Tuszynski, 2002; Kritzer, 2002; Sárvári et al., 2010; Mo et al., 2015). Expression of ERβ provides a mechanism for BLA PV cells to be regulated by ovarian hormones and across the estrous cycle. Alterations in PV cortical inhibition has been found to change across the estrous cycle and is dependent on ERβ (Clemens et al., 2019). Based on results from Clemens et al. (2019), it suggests BLA PV cells may be modulated in a similar mechanism. Therefore, characterization of BLA PV cells across the estrous cycle is needed if we want to determine how fluctuations in ovarian hormones influence PV cellular properties.

I first confirmed that most BLA PV cells were GABAergic by staining for GAD67, the primary enzyme responsible for converting glutamate to GABA (Soghomonian and Martin, 1998). My results corroborate findings from previous studies (McDonald and Mascagni, 2001; Mascagni and McDonald, 2003). The overwhelming majority of BLA PV cells expressed GAD67, and, thus, are GABAergic (Fig. 5).

In terms of the subpopulation of PV cells surrounded by PNNs, I found approximately 35% of PV cells were ensheathed by PNNs, suggesting that 65% of PV cells are not surrounded by PNNs (Fig. 5). Although Morikawa et al. (2017) only quantified the percentage of PV cells enwrapped by PNNs in the basal nucleus, they found a large population of PV neurons in the medial and caudal portions of the basal nucleus are not surrounded by PNNs, supporting my

finding that most PV cells in the BLA are not ensheathed by PNNs. Additionally, my data suggest the density of PV/PNNs cells is not influenced by sex or estrous cycle stage. Several studies examining PV/PNN expression have included males and females, but have failed to comment on whether sex differences existed (Chu et al., 2018; Drzewiecki et al., 2020; Richardson et al., 2021). Only a few studies have examined differences in BLA PV/PNN expression between males and females. For example, Gildawie et al. (2020) found no main effect of sex on the density of BLA PV, PNNs, non-PV PNNs, or PV/PNNs in adult male and female mice that underwent maternal separation from 2-20 days of age. Although Zhang et al. (2021) did not examine the BLA or the density of PV cells, they found no effect of sex or gonadal hormones on the density of PNNs in various hypothalamic nuclei, including the paraventricular hypothalamic nucleus, lateral hypothalamus, or ventromedial hypothalamic nucleus. Similarly, Griffiths et al. (2019) found no sex difference in the mean count of adult PV, PNN, and PV/PNN cells in the CA1 region of the hippocampus or the neocortex. Ciccarelli et al. (2020) is one of the few studies to discover a sex difference in the staining of adult PNNs in the posterodorsal medial amygdala, ventral premammillary nucleus, and medial tuberal nucleus; the staining of PNNs was higher in males compared to females. They suggested PNN-expression sexual dimorphism was linked to brain regions involved in reproduction, rather than the adjacent defensive network (Ciccarelli et al., 2020). However, I believe this explanation warrants further investigation as Zhang et al. (2021) found no effect of sex in nuclei known to be involved in reproduction. Overall, my results are in concordance with the literature, suggesting the density of adult BLA PV/PNNs is not influenced by biological sex.

Relatively little data exists on the effect of estrous cycle on PV/PNN expression. Uriarte et al. (2020) saw no PNNs in the medial preoptic area (mPOA) of naturally cycling female rats in

diestrus, proestrus, or estrus. However, the lack of PNNs in the mPOA seems to be specific to the brain region, as Seeger et al. (1994) also did not detect PNNs in the mPOA of male and virgin female rats. Recently, Blake et al. (2022, Prepint) examined the effects of early-life adversity on PV/PNN expression in adult female mice across the estrous cycle. They found the density of PNNs and PV/PNNs in the ventral dentate gyrus (vDG) was higher during estrous than diestrus in control mice; however, this finding did not apply to the ventral CA1 region (Blake et al., 2022, Preprint). Additionally, they did not find an effect of estrous cycle on PV cell density in the vDG or vCA1, which is similar to what Torres-Reveron et al. (2009) found (Blake et al., 2002, Preprint). These results suggest estrous cycle differences in PV/PNN density is dependent upon the brain region. Based upon my results, I can conclude fluctuations in ovarian hormones do not influence the density of PV/PNNs in the BLA.

When examining BLA PV-IRES-Cre recombination efficiency and specificity, I found a low recombination efficiency, but high specificity in both males and females. I assessed recombination by crossing PV-IRES-Cre mice, in which Cre recombinase expression is driven by the PV promoter, to Rosa-CAG-LSL-tdTomato-WPRE mice, in which tdTomato expression is gated by a lox-stop-lox cassette. In doing so, PV-expressing cells were selectively labeled by tdTomato. To examine Cre recombination efficiency, I determined the ratio of PV cells that expressed tdTomato. I found that approximately 43% of PV cells expressed tdTomato, suggesting that 57% of PV cells did not undergo recombination (Fig. 5). Similarly, to assess Cre recombination specificity, I examined the proportion of tdTomato that expressed PV and found a 91% specificity rate; however, roughly 80% of tdTomato cells expressed GAD67 and co-expressed PV and GAD67 (Fig. 5). My values for PV-IRES-Cre recombination efficiency and specificity are similar to what previous studies have reported. Lucas et al. (2016) found 30% of BLA PV neurons

exhibited recombination while 90% of recombined cells were GABAergic PV cells in peripubertal males. Nigro et al. (2021) similarly reported a 44% efficiency and 95% specificity rate in the perirhinal cortex.

Although the Nigro et al. (2021) assessed recombination in males and females, they did not stratify their data by sex. While most of the recombined subpopulations did not differ by sex or estrous cycle, I did find a sex difference in the percentage of tdTomato cells expressing GAD67 and PV/GAD67, where the ratios were lower in females compared to males. Additionally, the ratio of PNNs surrounding PV cells expressing GAD67 was also lower in females than males. While the PNN statistic does not involve the recombined population, it is interesting that the PV/GAD67 subpopulation of tdTomato cells and PNNs is lower in females compared to males. The mechanism driving the decreased density in females is unknown. It is possible that Cre recombination may be decreasing GAD67 density in females only in specific cellular populations. Cre recombination is known to alter physiological properties of cells from inducing non-targeted recombination to decreasing cell growth and causing DNA damage (Matthaei, 2007; Harno, et al., 2013). Schmidt-Supprian and Rajewsky (2007) explains Cre recombinase may affect expression of genes at or near the site of recombination. Though this does not apply to current findings since genes encoding PV and GAD67 are on different chromosomes. Whether the effects found are biologically significant remains; slight differences in tissue processing or imaging between males and females may have impacted quantification. Taking a closer examination of GAD67-expressing cells or staining with another GABAergic marker, such as GABA, can revel if the sex differences truly exist. Overall, my study is the first to determine PV-IRES-Cre recombination independently in both males and females. My finding that recombination is essentially equivalent between sexes is noteworthy. It suggests future studies can reliably use PV-IRES-Cre mice to study sex differences dependent on

Cre recombination in the BLA. Therefore, any sex differences observed is not due to disparities in recombination.

While all my results are based on the density of cellular subpopulations within the BLA, there are other aspects to consider, such as intensity and somatic size. Cellular intensity correlates to relative levels of protein expression whereas somatic size can reveal insight into a cell's physiological properties (Savage et al., 2007; Shihan et al., 2021). As stated above, Blume et al. (2017) found an increase in the amount of BLA PV-expressing cells in males compared to females and in diestrus compared to proestrus females from rats. I did not replicate the results determined by Blume et al. (2017). They suggested the sex and cycle dependent differences in BLA PV density may reflect alternations in PV activity, rather than generation of new neurons (Blume et al., 2017). PV expression is known to change based on activity and experience (Patz et al., 2004; Donato et al., 2013; Dehorter et al., 2015; Santiago et al., 2018). High PV expression is known to increase calcium buffering capacity and influences GABA release from these cells (Guadagno et al. 2021). In support of this, Donato et al. (2013) found PV intensity is positively correlated to GAD67 intensity, suggesting higher PV expression is associated with increased expression of GAD67. Moreover, PV cells surrounded by PNNs exhibit higher PV expression and larger cell bodies compared to PV cells not ensheathed by PNNs (Enwright et al., 2016; McDonald et al., 2018). Differences in PV activity may therefore explain the discrepancy between my findings and those found by Blume et al. (2017).

Despite the lack of sex or estrous cycle differences in cellular density, it is still unknown whether the intensity and cell body size of BLA PV cells surrounded by PNNs is influenced by the rodent estrous cycle. Further examination of the PV cellular population in the BLA is warranted for many reasons. These cells are regulated differently between sexes and across the estrous cycle

(Blume et al., 2017). Additionally, alternations in PV cells and dysregulation of GABAergic function in the BLA have been implicated in affective disorders, including anxiety and major depressive disorder, which have a higher prevalence in women than men (Altemus et al., 2014; Sharp 2017; Perlman et al., 2021).

References

1. Aggleton, J.P., and Mishkin, M. (1986). The amygdala: Sensory gateway to the emotions. In Plutchik, R., and Kellerman, H. (Eds.), Vol. 3. Emotion: Theory, research and experience (pp. 281–299). New York: Academic Press.

2. Ajayi, A.F., and Akhigbe, R.E. (2020). Staging of the estrous cycle and induction of estrus in experimental rodents: An update. Fertil Res Pract. 6:5. doi: 10.1186/s40738-020-00074-3

3. Allen, E., Francis, B.F., Robertson, L.L., Colgate, C.E., Johnston, C.G., Doisy, E.A., et al. (1924). The hormone of the ovarian follicle; its localization and action in test animals, and additional points bearing upon the internal secretion of the ovary. Am J Anat. 34:133-18. doi: 10.1002/aja.1000340104

4. Altemus, M., Sarvaiya, N., and Epperson, N.C. (2014). Sex differences in anxiety and depression clinical perspectives. Front Neuroendocrinol. 35(3):320-30. doi: 10.1016/j.yfrne.2014.05.004

5. Baker, K.D., Gray, A.R., and Richardson, R. (2017). The development of perineuronal nets around parvalbumin gabaergic neurons in the medial prefrontal cortex and basolateral amygdala of rats. Behav Neurosci. 131(4):289-303. doi: 10.1037/bne0000203

6. Balmer, T.S. (2016). Perineuronal nets enhance the excitability of fast-spiking neurons. eNeuro. 3(4):ENEURO.0112-16.2016. doi: 10.1523/ENEURO.0112-16.2016

7. Blake, J.L., Sahana, S.M., Hanani, M., Clappier, M., Boyer, S., Vasquez, B., et al. (2022). The estrous cycle modulates early-life adversity effects on mouse avoidance behavior through progesterone signaling. bioRxiv. 2022.02.23.481634. doi: 10.1101/2022.02.23.481634

8. Blume, S.R., Freedberg, M., Vantrease, J.E., Chan, R., Padival, M., Record, M.J., et al. (2017). Sex- and estrus-dependent differences in rat basolateral amygdala. J Neurosci. 37:10567-10586. doi: 10.1523/JNEUROSCI.0758-17.2017

9. Blurton-Jones, M., and Tuszynski, M.H. (2002). Estrogen receptor-beta colocalizes extensively with parvalbumin-labeled inhibitory neurons in the cortex, amygdala, basal forebrain, and hippocampal formation of intact and ovariectomized adult rats. J Comp Neurol. 452(3):276-87. doi: 10.1002/cne.10393

10. Butcher, R.L., Collins, W.E., and Fugo, N.W. (1974). Plasma concentration of LH, FSH, prolactin, progesterone and estradiol-17B throughout the 4-day estrous cycle of the rat. Endocrinol. 94(6):1704-1708. doi: 10.1210/endo-94-6-1704

11. Carulli, D., and Verhaagen, J. (2021). An extracellular perspective on CNS maturation: Perineuronal nets and the control of plasticity. Int J Mol Sci. 22:2434. doi: 10.3390/ijms22052434

12. Ciccarelli, A., Weijers, D., Kwan, W., Warner, C., Bourne, J., and Gross. C.T. (2020). Sexually dimorphic perineuronal nets in the rodent and primate reproductive circuit. J Comp Neurol. 529(13):3274-3291. doi: 10.1002/cne.25167

13. Chu, P., Abraham, R., Budhu, K., Khan, U., De Marco Garcia, N., and Brumberg, J.C. (2018). The impact of perineuronal net digestion using chondroitinase ABC on the intrinsic physiology of cortical neurons. Neurosci. 388:23-35. doi: 10.1016/j.neuroscience.2018.07.004

14. Clemens, A.M., Lenschow, C., Beed, P., Li, L., Sammons, R., Naumann, R.K., et al. (2019). Estrus-cycle regulation of cortical inhibition. Curr Biol. 29(4):605-615.e6. doi: 10.1016/j.cub.2019.01.045

15. Cora, M.C., Kooistra, L., and Travlos, G. (2015). Vaginal cytology of the laboratory rat and mouse: Review and criteria for the staging of the estrous cycle using stained vaginal smears. Toxicol Pathol. 43(6):776-93. doi: 10.1177/0192623315570339

16. Deepa, S.S., Umehara, Y., Higashiyama, S., Itoh, N., and Sugahara, K. (2002). Specific molecular interactions of oversulfated chondroitin sulfate E with various heparin-binding growth factors. Implications as a physiological binding partner in the brain and other tissues. J Biol Chem. 277:43707–43716. doi: 10.1074/jbc.M207105200

17. Dehorter, N., Ciceri, G., Bartolini, G., Lim, L., del Pino, I., and Marín, O. (2015). Tuning of fast-spiking interneuron properties by an activity-dependent transcriptional switch. Sci. 349(6253):1216-20. doi: 10.1126/science.aab3415

18. Donato, F., Rompani, S.B., and Caroni, P. (2013). Parvalbumin-expressing basket-cell network plasticity induced by experience regulates adult learning. Nature. 504(7479):272-6. doi: 10.1038/nature12866

19. Drzewiecki, C.M., Willing, J., and Juraska, J.M. (2020). Influences of age and pubertal status on number and intensity of perineuronal nets in the rat medial prefrontal cortex. Brain Struct Funct. 225:2495–2507. doi: 10.1007/s00429-020-02137-z

20. Dityatev, A., Brückner, G., Dityateva, G., Grosche, J., Kleene, R., and Schachner, M. (2007). Activity-dependent formation and functions of chondroitin sulfate-rich extracellular matrix of perineuronal nets. Dev Neurobiol. 67(5):570-88. doi: 10.1002/dneu.20361

21. Enwright, J.F., Sanapala, S., Foglio, A., Berry, R., Fish, K.N., and Lewis, D.A. (2016). Reduced labeling of parvalbumin neurons and perineuronal nets in the dorsolateral prefrontal cortex of subjects with schizophrenia. Neuropsychopharmacol. 41(9):2206-14. doi: 10.1038/npp.2016.24

22. Favuzzi, E., Marques-Smith, A., Deogracias, R., Winterflood, C.M., Sánchez-Aguilera, A., Mantoan, L., et al. (2017). Activity-dependent gating of parvalbumin interneuron function by the perineuronal net protein brevican. Neuron. 95(3):639-655.e10. doi: 10.1016/j.neuron.2017.06.028

23. Ferguson, B.R., and Gao, W.J. (2018). PV interneurons: critical regulators of E/I balance for prefrontal cortex-dependent behavior and psychiatric disorders. Front Neural Circuits. 12:37. doi: 10.3389/fncir.2018.00037

24. Filice, F., Celio, M.R., Babalian, A., Blum, W., and Szabolcsi, V. (2017). Parvalbumin-expressing ependymal cells in rostral lateral ventricle wall adhesions contribute to aging-related ventricle stenosis in mice. J Comp Neurol. 525:3266–3285. doi: 10.1002/cne.24276

25. Freeman, M. E. (1994). The neuroendocrine control of the ovarian cycle of the rat. In Knobil, E., and Neill, J. (Eds.), Vol. 2. The physiology of reproduction (pp.613-658). New York: Raven Press.

26. Frischknecht, R., Heine, M., Perrais, D., Seidenbecher, C. I., Choquet, D., and Gundelfinger, E. D. (2009). Brain extracellular matrix affects AMPA receptor lateral mobility and short-term synaptic plasticity. Nat Neurosci. 12:897–904. doi: 10.1038/nn.2338

27. Galtrey, C.M., and Fawcett, J.W. (2007). The role of chondroitin sulfate proteoglycans in regeneration and plasticity in the central nervous system. Brain Res Rev. 54:1–18. doi: 10.1016/j.brainresrev.2006.09.006

28. Gildawie, K.R., Honeycutt, J.A., and Brenhouse, H.C. (2020). Region-specific effects of maternal separation on perineuronal net and parvalbumin-expressing interneuron formation in male and female rats. Neurosci. 428:23-37. doi: 10.1016/j.neuroscience.2019.12.010

29. Gogolla, N., Caroni, P., Lüthi, A., and Herry, C. (2009). Perineuronal nets protect fear memories from erasure. Sci. 325(5945):1258-61. doi: 10.1126/science.1174146

30. Griffiths, B.B., Madden, A., Edwards, K.A., Zup, S.L., and Stary, C. M. (2019). Age-dependent sexual dimorphism in hippocampal cornu ammonis-1 perineuronal net expression in rats. Brain Behav. 9(5):e01265. doi: 10.1002/brb3.1265

31. Guadagno, A., Belliveau, C., Mechawar, N., and Walker, C.D. (2021). Effects of early life stress on the developing basolateral amygdala-prefrontal cortex circuit: The emerging role of local inhibition and perineuronal nets. Front Hum Neurosci. 15:669120. doi: 10.3389/fnhum.2021.669120

32. Harno, E., Cottrell, E.C., and White, A. (2013). Metabolic pitfalls of CNS Cre-based technology. Cell Metab. 18(1):21-8. doi: 10.1016/j.cmet.2013.05.019

33. Härtig, W., Brauer, K., and Brückner, G. (1992). Wisteria floribunda agglutinin-labelled nets surround parvalbumin-containing neurons. Neuroreport. 3:869–872. doi: 10.1097/00001756-199210000-00012

34. Härtig, W., Derouiche, A., Welt, K., Brauer, K., Grosche, J., Mäder, M., et al. (1999). Cortical neurons immunoreactive for the potassium channel Kv3.1b subunit are predominantly surrounded by perineuronal nets presumed as a buffering system for cations. Brain Res. 842:15–29. doi: 10.1016/s0006-8993(99)01784-9

35. Hippenmeyer, S., Vrieseling, E., Sigrist, M., Portmann, T., Laengle, C., Ladle, D.R., et al. (2005). A developmental switch in the response of DRG neurons to ETS transcription factor signaling. PLoS Biol. 3(5):e159. doi: 10.1371/journal.pbio.0030159

36. Johnston, J.B. (1923). Further contributions to the study of the evolution of the forebrain. J Comp Neurol. 35:371–482. doi: 10.1002/cne.900350502

37. Kritzer, M.F. (2002). Regional, laminar, and cellular distribution of immunoreactivity for ER alpha and ER beta in the cerebral cortex of hormonally intact, adult male and female rats. Cereb Cortex. 12(2):116-28. doi: 10.1093/cercor/12.2.116

38. Kuiper, G.G., Enmark, E., Pelto-Huikko, M., Nilsson, S., and Gustafsson, J.A. (1996). Cloning of a novel receptor expressed in rat prostate and ovary. Proc Natl Acad Sci U.S.A. 93(12):5925–5930. doi: 10.1073/pnas.93.12.5925

39. Kurokawa, T., Tsuda, M., and Sugino, Y. (1976). Purification and characterization of a lectin from Wisteria floribunda seeds. J Biol Chem. 251:5686–5693. doi:10.1016/s0021-9258(17)33112-5

40. LeDoux, J.E., Cicchetti, P., Xagoraris, A., and Romanski, L.M. (1990). The lateral amygdaloid nucleus: Sensory interface of the amygdala in fear conditioning. Neurosci. 10(4):1062-9. doi: 10.1523/JNEUROSCI.10-04-01062.1990

41. Lucas, E.K., and Clem, R.L. (2018). GABAergic interneurons: The orchestra or the conductor in fear learning and memory? Brain Res Bull. 141:13-19. doi: 10.1016/j.brainresbull.2017.11.016

42. Lucas, E.K., Jegarl, A.M., Morishita, H., and Clem, R.L. (2016). Multimodal and site-specific plasticity of amygdala parvalbumin interneurons after fear learning. Neuron. 91(3):629-43. doi: 10.1016/j.neuron.2016.06.032

43. Madisen, L., Zwingman, T.A., Sunkin, S.M., Oh, S.W., Zariwala, H.A., Gu, H., et al. (2010). A robust and high-throughput Cre reporting and characterization system for the whole mouse brain. Nat Neurosci. 13(1):133–140. doi: 10.1038/nn.2467

44. Mascagni, F., and McDonald, A.J. (2003). Immunohistochemical characterization of cholecystokinin containing neurons in the rat basolateral amygdala. Brain Res. 976: 171–184. doi: 10.1016/s0006-8993(03)02625-8

45. Matthaei, K.I. (2007). Genetically manipulated mice: A powerful tool with unsuspected caveats. J Physiol. 582(Pt 2):481-8. doi: 10.1113/jphysiol.2007.134908

46. McDonald, A.J. (1984). Neuronal organization of the lateral and basolateral amygdaloid nuclei in the rat. J Comp Neurol. 222(4):589-606. doi: 10.1002/cne.902220410

47. McDonald, A.J. (1991). Topographical organization of amygdaloid projections to the caudatoputamen, nucleus accumbens and related striatal-like areas of the rat brain. Neurosci. 44:15–33. doi: 10.1016/0306-4522(91)90248-m

48. McDonald, A.J. (1992). Projection neurons of the basolateral amygdala: A correlative Golgi and retrograde tract tracing study. Brain Res Bull. 28:179–185. doi: 10.1016/0361-9230(92)90177-y

49. McDonald, A.J. (1998). Cortical pathways to the mammalian amygdala. Prog Neurobiol. 55(3):257-332. doi: 10.1016/s0301-0082(98)00003-3

50. McDonald, A. J. (2020). Functional neuroanatomy of the basolateral amygdala: Neurons, neurotransmitters, and circuits. In Urban, J.H., and Rosenkranz, J.A. (Eds.), Vol. 26. Handbook of behavioral neuroscience (pp.1–38). London: Elsevier. doi: 10.1016/b978-0-12-815134-1.00001-5

51. McDonald, A.J., Hamilton, P.G., and Barnstable, C.J. (2018). Perineuronal nets labeled by monoclonal antibody VC1.1 ensheath interneurons expressing parvalbumin and calbindin in the rat amygdala. Brain Struct Funct. 223(3):1133-1148. doi: 10.1007/s00429-017-1542-8

52. McDonald, A.J., and Mascagni, F. (2001). Colocalization of calcium-binding proteins and GABA in neurons of the rat basolateral amygdala. Neurosci. 105(3):681-93. doi: 10.1016/s0306-4522(01)00214-7

53. McDonald, A.J., and Mott, D.D. (2021). Neuronal localization of m1 muscarinic receptor immunoreactivity in the monkey basolateral amygdala. J Comp Neurol. 529:2450-2463. doi: 10.1002/cne.25104

54. Mo, A., Mukamel, E.A., Davis, F.P., Luo, C., Henry, G.L., Picard, S., et al. (2015). Epigenomic signatures of neuronal diversity in the mammalian brain. Neuron. 86(6):1369-84. doi: 10.1016/j.neuron.2015.05.018

55. Morawski, M., Reinert, T., Meyer-Klaucke, W., Wagner, F. E., Tröger, W., Reinert, A., et al. (2015). Ion exchanger in the brain: Quantitative analysis of perineuronally fixed anionic binding sites suggests diffusion barriers with ion sorting properties. Sci Rep. 5:16471. doi: 10.1038/srep16471

56. Morena, M., Aukema, R.J., Leitl, K.D., Rashid, A.J., Vecchiarelli, H.A., Josselyn, S.A., et al. (2019). Upregulation of anandamide hydrolysis in the basolateral complex of amygdala reduces fear memory expression and indices of stress and anxiety. Neurosci. 39(7):1275-1292. doi: 10.1523/JNEUROSCI.2251-18.2018

57. Morikawa, S., Ikegaya, Y., Narita, M., and Tamura, H. (2017). Activation of perineuronal net-expressing excitatory neurons during associative memory encoding and retrieval. Sci Rep. 7:46024. doi: 10.1038/srep46024

58. Nigro, M.J., Kirikae, H., Kjelsberg, K., Nair, R.R., and Witter, M.P. (2021). Not all that is gold glitters: PV-IRES-Cre mouse line shows low efficiency of labeling of parvalbumin interneurons in the perirhinal cortex. Front Neural Circuits. 15:781928. doi: 10.3389/fncir.2021.781928

59. Pantazopoulos, H., Gisabella, B., Rexrode, L., Benefield, D., Yildiz, E., Seltzer, P., et al. (2020). Circadian rhythms of perineuronal net composition. eNeuro. 7(4):ENEURO.0034-19.2020. doi: 10.1523/ENEURO.0034-19.2020

60. Pantazopoulos, H., Woo, T.U., Lim, M.P., Lange, N., and Berretta, S. (2010). Extracellular matrix-glial abnormalities in the amygdala and entorhinal cortex of subjects diagnosed with schizophrenia. Arch Gen Psychiatry. 67:155–166. doi: 10.1001/archgenpsychiatry.2009.196

61. Perlman, G., Tanti, A., and Mechawar, N. (2021). Parvalbumin interneuron alterations in stress-related mood disorders: A systematic review. Neurobiol Stress. 15:100380. doi: 10.1016/j.ynstr.2021.10 10.1016/j.ynstr.2021.100380

62. Patz, S., Grabert, J., Gorba, T., Wirth, M.J., and Wahle P. (2004). Parvalbumin expression in visual cortical interneurons depends on neuronal activity and TrkB ligands during an early period of postnatal development. Cereb Cortex. 14(3):342-51. doi: 10.1093/cercor/bhg132

63. Richardson, R., Bowers, J., Callaghan, B.L., and Baker, K.D. (2021). Does maternal separation accelerate maturation of perineuronal nets and parvalbumin-containing inhibitory interneurons in male and female rats? Dev Cogn Neurosci. 47:100905. doi: 10.1016/j.dcn.2020.100905

64. Sah, P., Faber, E.S., Lopez De Armentia, M., and Power, J. (2003). The amygdaloid complex: Anatomy and physiology. Physiol Rev. 83(3):803-34. doi: 10.1152/physrev.00002.2003.

65. Santiago, A.N., Lim, K.Y., Opendak, M., Sullivan, R.M., and Aoki, C. (2018). Early life trauma increases threat response of peri-weaning rats, reduction of axo-somatic synapses formed by parvalbumin cells and perineuronal net in the basolateral nucleus of amygdala. J Comp Neurol. 526(16):2647–2664. doi: 10.1002/cne.24522

66. Sárvári, M., Hrabovszky, E., Kalló, I., Galamb, O., Solymosi, N., Likó, I., et al. (2010). Gene expression profiling identifies key estradiol targets in the frontal cortex of the rat. Endocrinol. 151(3):1161-76. doi: 10.1210/en.2009-0911

67. Savage, V.M., Allen, A.P., Brown, J.H., Gillooly, J.F., Herman, A.B., Woodruff, W.H., et al. (2007). Scaling of number, size, and metabolic rate of cells with body size in mammals. PNAS. 104(11):4718-4723. doi: 10.1073/pnas.0611235104

68. Schmidt-Supprian, M., and Rajewsky, K. (2007). Vagaries of conditional gene targeting. Nat Immunol. 8(7):665-8. doi: 10.1038/ni0707-665

69. Seeger, G., Brauer, K., Härtig, W., and Brückner, G. (1994). Mapping of perineuronal nets in the rat brain stained by colloidal iron hydroxide histochemistry and lectin cytochemistry. Neurosci. 58(2):371-88. doi: 10.1016/0306-4522(94)90044-2

70. Sharp, B. (2017). Basolateral amygdala and stress-induced hyperexcitability affect motivated behaviors and addiction. Transl Psychiatry. 7:e1194. doi: 10.1038/tp.2017.161

71. Shihan, M.H., Novo, S.G., Le Marchand, S.J., Wang, Y., and Duncan, M.K. (2021). A simple method for quantitating confocal fluorescent images. Biochem Biophys Rep. *25*:100916. doi: 10.1016/j.bbrep.2021.100916

72. Smith, M.S., Freeman, M.E., and Neill, J.D. (1975). The control of progesterone secretion during the estrous cycle and early pseudopregnancy in the rat: Prolactin, gonadotropin and steroid levels associated with rescue of the corpus luteum of pseudopregnancy. Endocrinol. 96(1):219–226. doi: 10.1210/endo-96-1-219

73. Soghomonian, J.J., and Martin, D.L. (1998). Two isoforms of glutamate decarboxylase: Why? Trends Pharmacol Sci. 19(12):500-5. doi: 10.1016/s0165-6147(98)01270-x

74. Sorg, B.A., Berretta, S., Blacktop, J.M., Fawcett, J.W., Kitagawa, H., Kwok, J.C., et al. (2016). Casting a wide net: Role of perineuronal nets in neural plasticity. Neurosci. 36(45):11459–11468. doi: 10.1523/JNEUROSCI.2351-16.2016

75. Torres-Reveron, A., Williams, T.J., Chapleau, J.D., Waters, E.M., McEwen, B.S., Drake, C.T., et al. (2009). Ovarian steroids alter mu opioid receptor trafficking in hippocampal parvalbumin GABAergic interneurons. Exp Neurol. 219(1):319–327. doi: 10.1016/j.expn 10.1016/j.expneurol.2009.06.001

76. Zhang, N., Yan, Z., Liu, H., Yu, M., He, Y., Liu, H., et al. (2021). Hypothalamic perineuronal nets are regulated by sex and dietary interventions. Front Physiol. 12:714104. doi: 10.3389/fphys.2021.714104

77. Uriarte, N., Ferreño, M., Méndez, D., and Nogueira, J. (2020). Reorganization of perineuronal nets in the medial preoptic area during the reproductive cycle in female rats. Sci Rep. 10(1):5479. doi: 10.1038/s41598-020-62163-z

Table 1. Antibodies, lectins, and dilutions used in this study.

Target	Host	Immunogen/Label	Clonality	Isotype	Dilution	Company (Cat. #)	RRID
Primary antibody							
PV	Rabbit	Recombinant rat PV	Poly	Antiserum	1:1000	Swant (PV27)	AB_2631173
GAD67	Mouse	Recombinant GAD67 protein	Mono	IgG2a	1:500	Millipore (MAB5406)	AB_2278725
Primary lectin							
WFL		*N*-Acetylgalactosamine			1:100	Vector Labs (B-1355-2)	
Secondary antibody							
Rabbit	Donkey	Alexa Fluor 647	Poly	IgG	1:500	Jackson (711-605-152)	AB_2492288
Mouse	Donkey	DyLight 405	Poly	IgG	1:200	Jackson (715-475-150)	AB_2340839
Secondary lectin							
Biotin		Streptavidin conjugated Alexa Fluor 488			1:100	Jackson (016-540-084)	

Abbreviations: parvalbumin (PV), glutamic acid decarboxylase 67 (GAD67), *Wisteria floribunda* lectin (WFL).

Table 2. Density (cell count/mm^2) of single, double, triple, and quadruple-labeled cells in the basolateral amygdala from males (n = 7), females (n = 11), females in diestrus 1 (n = 4), and females in proestrus (n = 7), shown as mean ± SEM.

Cellular Population	**Males**	**Females**	**Diestrus 1**	**Proestrus**
tdTomato	61.00 ± 8.33	62.77 ± 4.43	58.13 ± 6.98	65.42 ± 5.86
PV	131.15 ± 5.64	131.27 ± 3.78	128.99 ± 4.94	132.58 ± 5.45
tdTomato/PV	56.70 ± 7.24	56.28 ± 3.55	51.44 ± 4.72	59.05 ± 4.80
tdTomato/GAD67	53.39 ± 7.53	51.47 ± 3.99	47.58 ± 6.32	53.69 ± 5.30
PV/GAD67	118.77 ± 6.20	114.34 ± 4.25	112.76 ± 2.77	115.25 ± 6.68
tdTomato/PV/GAD67	51.08 ± 6.87	48.39 ± 3.52	44.89 ± 4.95	50.39 ± 4.85
PNNs	90.89 ± 2.60	95.04 ± 2.57	92.62 ± 3.63	96.42 ± 3.55
tdTomato/PNNs	29.93 ± 2.27	28.84 ± 1.83	29.57 ± 1.65	28.42 ± 2.81
PV/PNNs	47.24 ± 2.85	44.71 ± 2.05	45.42 ± 2.51	44.31 ± 3.02
Non-PV/PNNs	43.66 ± 3.97	50.33 ± 2.94	47.20 ± 4.96	52.11 ± 3.76
tdTomato/PV/PNNs	29.00 ± 2.22	27.49 ± 1.93	27.33 ± 1.85	27.59 ± 2.96
PV/GAD67/PNNs	43.05 ± 1.97	39.61 ± 2.20	40.11 ± 1.74	39.33 ± 3.43
tdTomato/PV/GAD67/PNNs	26.54 ± 1.98	24.02 ± 2.07	23.99 ± 1.62	24.04 ± 3.24

Abbreviations: parvalbumin (PV), glutamic acid decarboxylase 67 (GAD67), perineuronal nets (PNNs).

Table 3. Percentage of PV cells that express GAD67, PNNs, and GAD67/PNNs, and the percentage of PNNs that surround non-PV cells, PV cells, and PV cells expressing GAD67 in the basolateral amygdala from males (n = 7), females (n = 11), females in diestrus 1 (n = 4), and females in proestrus (n = 7), shown as mean ± SEM. The %PNNs that surround PV/GAD67 cells was lower in females compared to males; two-tailed, unpaired t-test ($t_{16} = 2.146$, $^*p < 0.05$).

		Males	**Females**	**Diestrus 1**	**Proestrus**
%PV	GAD67	90.19 ± 1.85	86.79 ± 1.56	87.54 ± 2.17	86.36 ± 2.23
	PNNs	37.90 ± 2.91	34.31 ± 1.46	35.82 ± 1.31	33.44 ± 2.17
	GAD67/PNNs	34.38 ± 2.05	30.32 ± 1.59	31.40 ± 0.75	29.70 ± 2.51
%PNNs	Non-PV	47.04 ± 3.36	53.11 ± 2.17	50.91 ± 3.63	54.37 ± 2.79
	PV	52.96 ± 3.36	46.89 ± 2.17	49.09 ± 3.63	45.63 ± 2.79
	PV/GAD67	48.17 ± 2.32	41.18 ± 2.13*	42.95 ± 2.57	40.17 ± 3.09

Abbreviations: parvalbumin (PV), glutamic acid decarboxylase 67 (GAD67), perineuronal nets (PNNs).

Table 4. Proportion of tdTomato cells, PV cells, and PNNs that express double, triple, and quadruple-labeled markers in the basolateral amygdala from males (n = 7), females (n = 11), females in diestrus 1 (n = 4), and females in proestrus (n = 7), shown as mean ± SEM. The %tdTomato cells that express GAD67 (t_{16} = 2.145, *p < 0.05) and PV cells that express GAD67 (t_{16} = 2.195, *p < 0.05) was lower in females compared to males; two-tailed, unpaired *t*-test.

		Males	**Females**	**Diestrus 1**	**Proestrus**
%tdTomato	PV	93.80 ± 1.31	90.17 ± 1.85	89.58 ± 4.05	90.51 ± 2.07
	GAD67	87.65 ± 1.84	81.89 ± 1.79*	81.47 ± 1.33	82.13 ± 2.80
	PV/GAD67	84.36 ± 1.65	77.44 ± 2.27*	77.56 ± 1.85	77.37 ± 3.53
	PNNs	52.26 ± 5.23	45.93 ± 2.29	51.61 ± 3.97	42.69 ± 2.11
	PV/PNNs	50.84 ± 5.51	43.48 ± 2.45	48.11 ± 5.14	40.84 ± 2.22
	PV/GAD67/PNNs	46.41 ± 4.36	38.04 ± 2.45	42.00 ± 3.52	35.78 ± 3.14
%PV	tdTomato	43.30 ± 4.14	42.74 ± 2.46	40.51 ± 4.02	44.02 ± 3.24
	tdTomato/GAD67	38.93 ± 3.90	36.56 ± 2.40	35.23 ± 4.18	37.32 ± 3.15
	tdTomato/PNNs	23.21 ± 1.76	20.90 ± 1.43	21.90 ± 1.51	20.32 ± 2.15
	tdTomato/GAD67/PNNs	21.23 ± 1.37	18.17 ± 1.51	18.99 ± 1.21	17.70 ± 2.34
%PNNs	tdTomato	33.56 ± 2.49	30.52 ± 1.86	32.33 ± 1.42	29.49 ± 2.82
	tdTomato/PV	32.55 ± 2.42	28.91 ± 1.99	29.84 ± 2.13	28.38 ± 2.99
	tdTomato/PV/GAD67	29.76 ± 2.03	25.05 ± 1.95	25.79 ± 1.33	24.63 ± 3.07

Abbreviations: parvalbumin (PV), glutamic acid decarboxylase 67 (GAD67), perineuronal nets (PNNs).

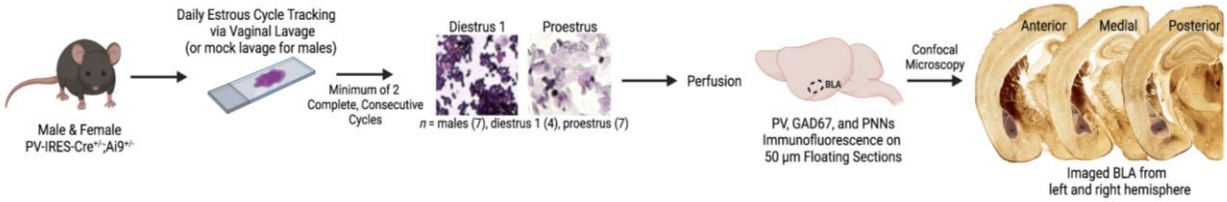

Figure 1. Experimental pipeline. Female PV-IRES-Cre$^{+/-}$;Ai9$^{+/-}$ mice underwent daily estrous cycle tracking via vaginal lavages for a minimum of 2 complete, consecutive cycles until they hit either diestrus 1 or proestrus. Male PV-IRES-Cre$^{+/-}$;Ai9$^{+/-}$ mice underwent daily mock lavages to account for the additional handling females received. Males (n = 7), diestrus females (n = 4), and proestrus females (n = 7) were perfused between 60-80 days of age. Immunofluorescence was conducted on 50 μm coronal sections by staining for parvalbumin (PV), glutamic acid decarboxylase 67 (GAD67), and perineuronal nets (PNNs). Using a confocal microscope, images were collected from the left and right hemisphere of an anterior, medial, and posterior section containing the basolateral amygdala (BLA).

Figure 2. Representative confocal microscopy images and density of cellular populations in the basolateral amygdala (BLA) of PV-IRES-Cre$^{+/-}$;Ai9$^{+/-}$ mice. (A-B) Representative confocal microscopy images of tdTomato-expressing cells (red) and immunofluorescence staining of PV (magenta), GAD67 (blue), and PNNs (green) in the BLA (large, dashed outline). Boxed portions (small, dashed outline) of the BLA in (A) are enlarged images in (B). Arrow heads in (B) signify triple-labeled cells. Scale bars: (A) 150 μm; (B) 50 μm. (C) The density (cell count/mm^2) of single, double, triple, and quadruple-labeled cells in the BLA from males (n = 7; black dots) and females (n = 11; red dots) combined, shown as mean ± SEM. Abbreviations: parvalbumin (PV), glutamic acid decarboxylase 67 (GAD67), perineuronal nets (PNNs).

A

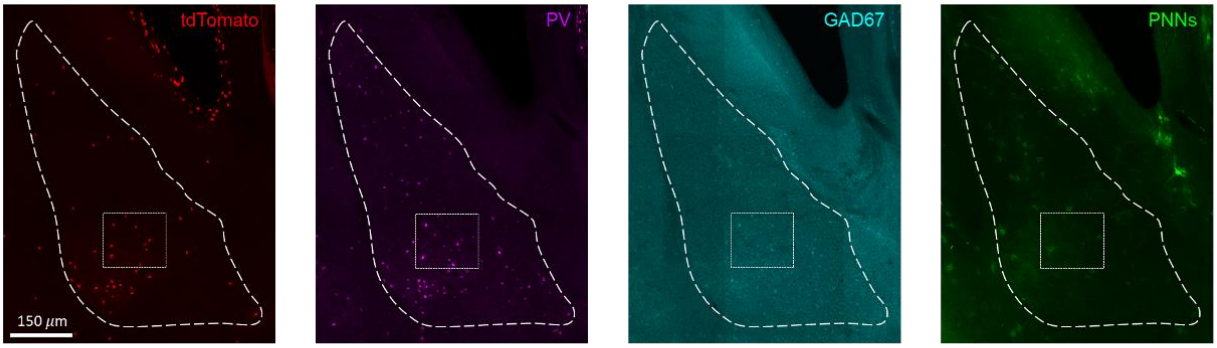
tdTomato
PV
GAD67
PNNs
150 μm

B

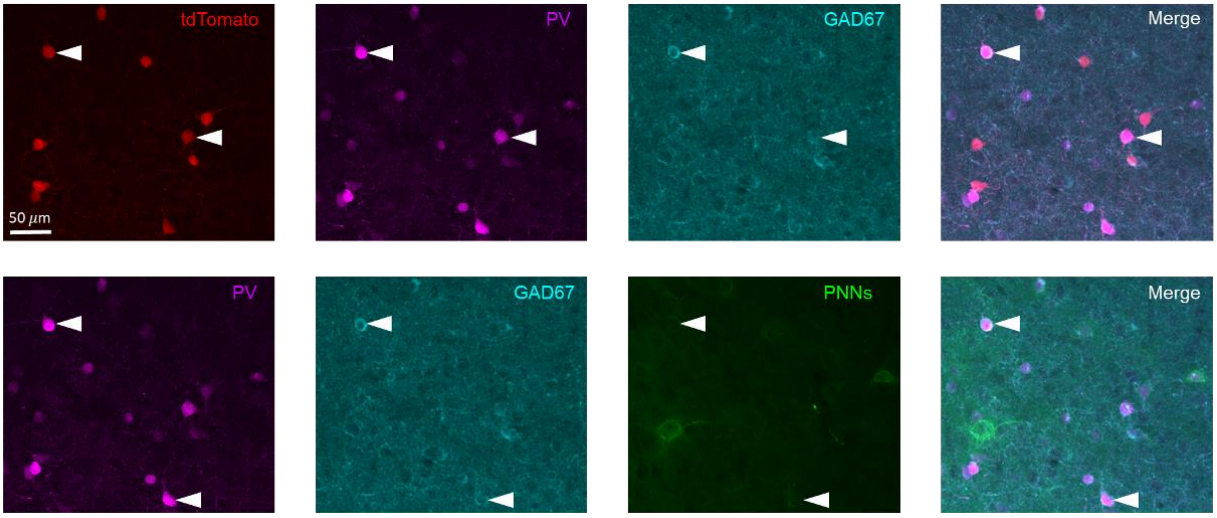
tdTomato
PV
GAD67
Merge
50 μm
PV
GAD67
PNNs
Merge

C

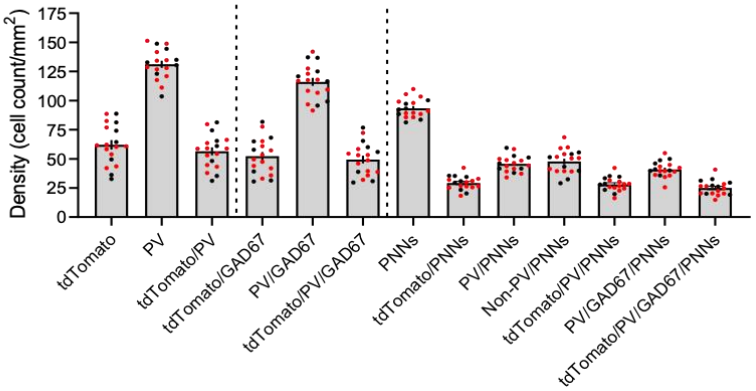
Density (cell count/mm2)
175
150
125
100
75
50
25
0
tdTomato
PV
tdTomato/PV
tdTomato/GAD67
PV/GAD67
tdTomato/PV/GAD67
PNNs
tdTomato/PNNs
PV/PNNs
Non-PV/PNNs
tdTomato/PV/PNNs
PV/GAD67/PNNs
tdTomato/PV/GAD67/PNNs

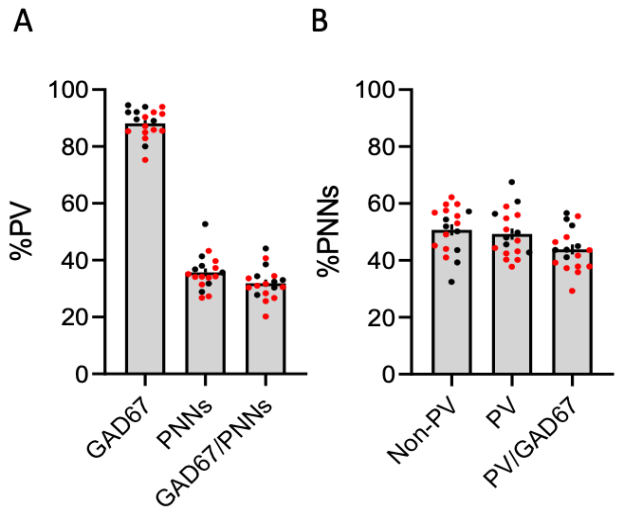

Figure 3. Proportion of PV cells and PNNs expressing double and triple-labeled markers. (A) Percentage of PV cells that express GAD67, PNNs, and GAD67/PNNs, and (B) the percentage of PNNs that surround non-PV, PV, and PV/GAD67 cells in the basolateral amygdala from males (*n* = 7; black dots) and females (*n* = 11; red dots) combined, shown as mean ± SEM. Abbreviations: parvalbumin (PV), glutamic acid decarboxylase 67 (GAD67), perineuronal nets (PNNs).

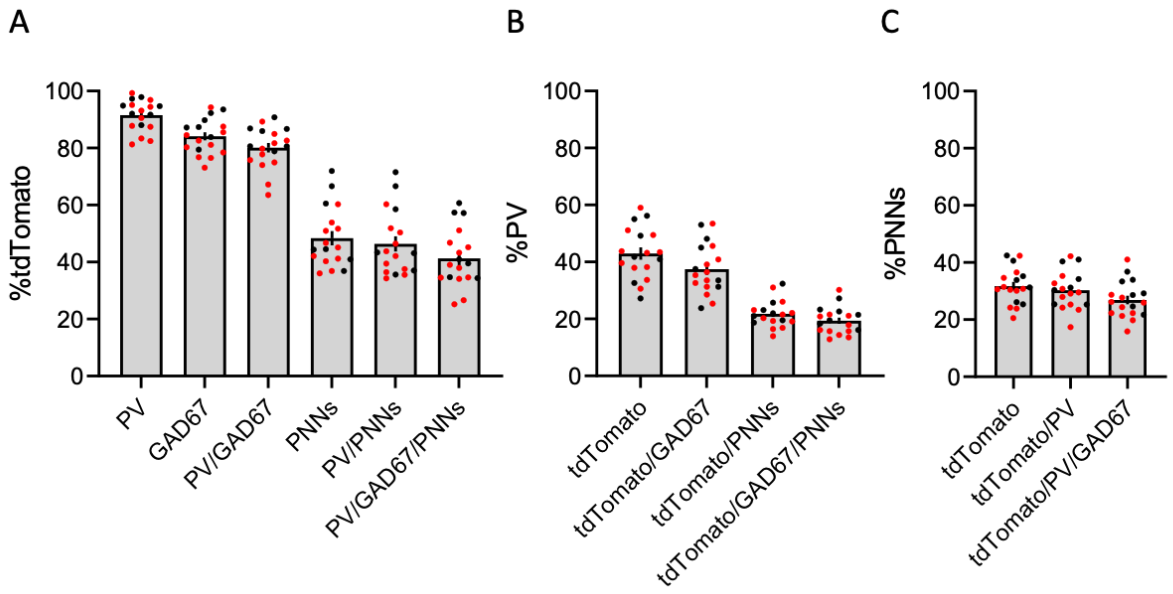

Figure 4. Proportion of tdTomato cells, PV cells, and PNNs expressing double, triple, and quadruple-labeled markers. (A) Percentage of tdTomato cells that express PV, GAD67, PV/GAD67, PNNs, PV/PNNs, and PV/GAD67/PNNs; (B) the percentage of PV cells that express tdTomato, tdTomato/GAD67, tdTomato/PNNs, and tdTomato/GAD67/PNNs; and (C) percentage of PNNs that surround tdTomato, tdTomato/PV, and tdTomato/PV/GAD67 cells in the basolateral amygdala from males (n = 7; black dots) and females (n = 11; red dots) combined, shown as mean ± SEM. Abbreviations: parvalbumin (PV), glutamic acid decarboxylase 67 (GAD67), perineuronal nets (PNNs).

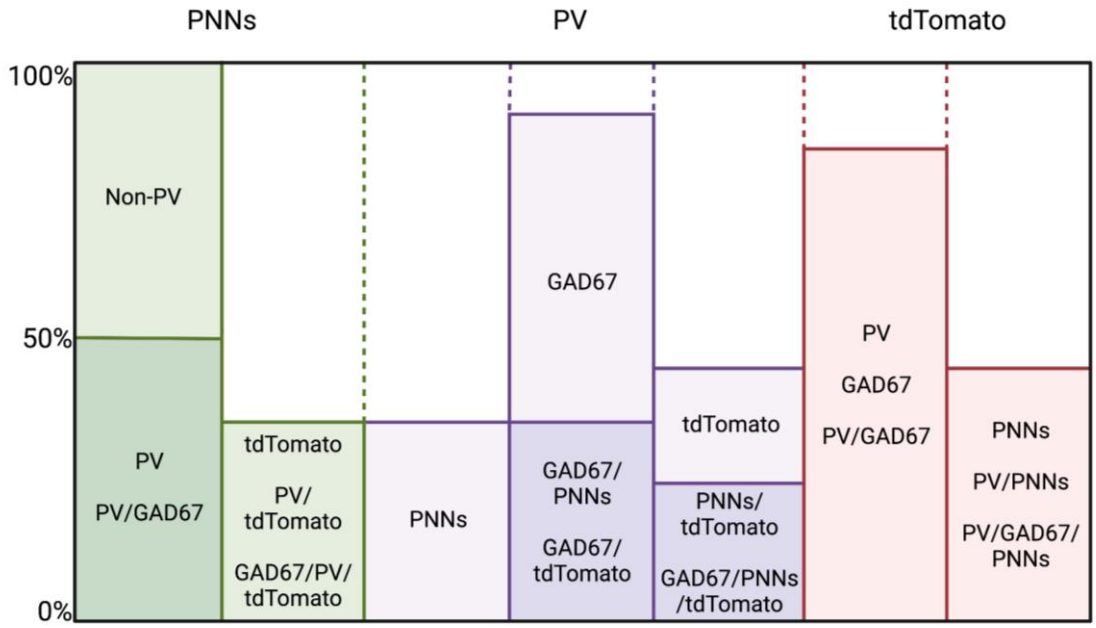

Figure 5. Summary of results depicting the relative percentages of PNNs (green), PV (purple), and tdTomato (red) co-expressing additional makers in the basolateral amygdala of males and females combined. Approximately 50% of PNNs surround PV cells that express GAD67 while the other 50% surround non-PV-expressing cells. Roughly 30% of PNNs surround cells co-expressing tdTomato, PV, and GAD67. Nearly 30% of PV cells are surrounded by PNNs. While 90% of PV cells express GAD67, approximately 30% of PV cells co-express GAD67 and PNNs or tdTomato cells. Only 40% of PV cells undergo Cre recombination and, thus, express tdTomato, indicating a low Cre recombination efficiency. Roughly 20% of PV cells co-express tdTomato, GAD67, and PNNs. About 80% of tdTomato cells express PV that also express GAD67, owning to high specificity of the PV-IRES-Cre mouse line. Nearly 40% of tdTomato cells co-express PV, GAD67, and PNNs. Abbreviations: parvalbumin (PV), glutamic acid decarboxylase 67 (GAD67), perineuronal nets (PNNs).